Received: 30 November 2021 | Revised: 6 April 2022 | Accepted: 6 April 2022

DOI: 10.1111/tbed.14555

Transboundary and Emerging Diseases

WILEY

ORIGINAL ARTICLE

Genetic characteristics and pathogenicity of the first bluetongue virus serotype 20 strain isolated in China

Yinglin Qi[1] | Fang Wang[1] | JiTao Chang[1] | Zhigang Jiang[1] | Chao Sun[1] | Jun Lin[2] | Jianmin Wu[2] | Li Yu[1]

[1]State Key Laboratory of Veterinary Biotechnology, Harbin Veterinary Research Institute, Chinese Academy of Agricultural Sciences, Harbin, China

[2]Guangxi Key Laboratory of Veterinary Biotechnology, Guangxi Veterinary Research Institute, Nanning, China

Correspondence
Li Yu, State Key Laboratory of Veterinary Biotechnology, Harbin Veterinary Research Institute, Chinese Academy of Agricultural Sciences, No. 678 Haping Road, Harbin 150069, Heilongjiang, China
Email: yuli02@caas.cn

Yinglin Qi and Fang Wang contributed equally to this study.

Funding information
National Natural Science Foundation of China, Grant/Award Numbers: 32102651, 31201941; Inner Mongolia Autonomous Region Major Science and Technology Project, Grant/Award Number: 2020ZD0006

Abstract

Bluetongue virus (BTV), a member of the genus *Orbivirus* in the family *Reoviridae*, is transmitted by biting midges and causes severe disease in domestic and wild ruminants. In the present study, a BTV strain, BTV-20/GX015/China/2013 (GX015), was isolated from sentinel cattle in Guangxi, China. Virus neutralization tests and phylogenetic analyses based on genomic segments 2 (S2) and 6 (S6) indicated that GX015 belongs to BTV serotype 20 (BTV-20) and represents a new topotype within BTV-20 strains, which makes GX015 the first BTV-20 strain isolated in China. Genomic analyses suggested that the 10 genomic segments of GX015 originated from a reassortment event, in which S2 and S6 are derived from exotic BTV-20 strains (South Africa or Australia), whereas the remaining eight genomic segments are apparently of Chinese origin and most likely share the same ancestor with a Taiwanese BTV-12 strain. Importantly, we evaluated the infectivity and pathogenicity of the BTV-20 strain in mice lacking the interferon receptor ($IFNAR^{-/-}$ mice, a good animal model for studying the pathogenesis, virulence and transmission of BTVs) and sheep for the first time, and found that GX015 causes severe disease and death in $IFNAR^{-/-}$ mice and clinical signs and viraemia in the natural host sheep. These results improve our understanding of the genetic characteristics, diversity and pathogenicity of BTVs, which is important for developing diagnostic methods and vaccines for the surveillance and prevention of bluetongue disease.

KEYWORDS
bluetongue virus (BTV), BTV-20, phylogeny, virulence, whole genome sequencing

1 | INTRODUCTION

Bluetongue virus (BTV), the aetiological agent of bluetongue disease (BT), infects both domestic and wild ruminants and is transmitted between mammalian hosts almost exclusively by biting midges (*Culicoides spp.*) (Maclachlan, 2011). BTV belongs to the *Orbivirus* genus of the *Reoviridae* family, and its genome comprises 10 segments (S1–S10) of double-stranded RNA (dsRNA) encoding seven structural proteins (VP1–VP7) and four non-structural proteins (NS1, NS2, NS3/NS3a and NS4). The existence of a fifth non-structural protein has also been suggested (Belhouchet et al., 2011; Ratinier et al., 2011; Stewart et al., 2015). BT has been reported on all continents except Antarctica. To date, a total of 32 distinct BTV serotypes (BTV-1 to BTV-24, atypical serotypes BTV-25 to BTV-29 and BTV-X to BTV-Z) have been identified, and several serotype-unassigned BTV strains have been isolated (Hofmann et al., 2008; Lorusso et al., 2018; Maan et al., 2011; Maan, et al., 2007; Marcacci et al., 2018; Savini et al., 2017; Yang et al., 2021; Zientara et al., 2014).

The main clinical signs of BT include fever, conjunctivitis, nasal discharge, oral erosions and ulcers, cyanotic tongue and lameness

(Darpel et al., 2007; Maclachlan, 2011). The severity of disease seems to depend on BTV strains, and the species and breed of susceptible animals involved. Severe clinical signs are generally confined to sheep and white-tailed deer, whereas goats and cattle occasionally exhibit clinical signs or remain largely asymptomatic and can act as reservoir hosts that remain viraemia for several months (Darpel et al., 2007). However, BTV-8 strains cause severe disease in cattle, including the typical clinical signs of BT, abortion, congenital deformities and cerebral abnormalities in a considerable number of offspring (Darpel et al., 2007; Elbers et al., 2008; Elbers, Backx, Meroc, et al., 2008; Wouda et al., 2008). BT outbreaks often result in severe economic consequences because of effects such as decreased milk production, reproductive losses, abortions, stillbirths and deaths, in addition to the costs of treatment, diagnosis, control measures and trade restriction (Rushton & Lyons, 2015). BT has been listed as a 'notifiable disease' by the World Organization for Animal Health (OIE).

To investigate the epidemics and distribution of insect-borne viruses in China, sentinel bovine herds were established in the Guangxi Zhuang Autonomous Region of China for an arbovirus surveillance study in 2013. In this study, a BTV-20 strain named BTV-20/GX015/China/2013 (abbreviated GX015) was first isolated in China. The whole genome of GX015 was characterized by sequencing and phylogenetic analyses. Additionally, we evaluated the infectivity and pathogenicity of the BTV-20 strain in mice lacking the interferon receptor ($IFNAR^{-/-}$) and sheep for the first time. The findings expand the BTV genome database, further improve our understanding of the genetic characteristics, pathogenicity and related public health aspects of BTVs, and provide clues for the prevention and control of BT.

2 | MATERIALS AND METHODS

2.1 | Virus isolation and detection

Whole-blood samples in EDTA collected from sentinel cattle in Guangxi were used for virus isolation. The C6/36 cell line derived from a mosquito was used for primary inoculation, and the supernatants and infected C6/36 cells were both used to inoculate the baby hamster kidney (BHK-21) cell line for blind passaging for three times (Sun et al., 2016; Yang et al., 2021). The infected BHK-21 cells that exhibited cytopathic effects of lysis and shedding were frozen and thawed three times, and after centrifugation, the supernatants were collected for viral identification and genomic sequencing. The harvested supernatants were processed for negative staining with 2% phosphotungstic acid and electron microscopy (EM) observation (Yang et al., 2021). An indirect immunofluorescence assay (IFA) was performed with an anti-BTV VP7 monoclonal antibody (Mab). Plaque morphology was also examined. BHK-21 monolayers were inoculated with the isolate, cultured under 1% methylcellulose overlay medium for 48 h, then fixed with methanol/acetone (1:1) and immunostained with the anti-BTV VP7 Mab (van Gennip et al., 2014). A virus neutralization test (VNT) was performed according to the descriptions reported by the OIE in 2016.

2.2 | Extraction of viral RNA and full-length amplification of cDNA

The supernatant was filtered using 0.22-μm filters and centrifuged at 50,000 *g* at 4°C for 30 min. Then, the pellet was suspended and treated with DNase (Promega) and RNase A (Promega). Viral RNA was extracted using TRI reagent (Sigma–Aldrich), and dsRNA was separated from single-stranded RNA by precipitation with 2 M LiCl (Sigma–Aldrich) at 4°C for 14 h. The dsRNA was subsequently precipitated by the addition of three volumes of 100% ethanol and 0.25 volumes of 7.5 M ammonium acetate. Sequence-independent cDNA synthesis and complete genome amplification were performed according to the full-length amplification of cDNA technique, as described previously (Maan, Rao, et al., 2007; Potgieter et al., 2009).

2.3 | Whole genome sequencing and phylogenetic analysis

PCR amplicons were directly used for sequencing, and each segment was sequenced twice to ensure accuracy of sequencing. The open reading frames of genomic segments were identified using EditSeq software (Lasergene version 7). Multiple alignments of consensus sequences for individual segments were performed using Clustal X (version 2) (Larkin et al., 2007). Pairwise distance calculations and phylogenetic tree constructions were performed with MEGA X (Kumar et al., 2018) using the maximum-likelihood (ML) method with full-length nucleotide (nt) sequences. The best-fit nucleotide substitution models for each segment were obtained based on the Bayesian Information Criterion (BIC), and the lowest BIC was used to undertake a ML analysis with 1000 bootstrap replicates. The 59 reference BTV sequences used for phylogenetic analysis in this study were downloaded from GenBank.

2.4 | Experimental infection of $IFNAR^{-/-}$ mice with GX015

The $IFNAR^{-/-}$ mice (AG129) was generously provided by Professor Jianping Zuo (Institut Pasteur of Shanghai, Chinese Academy of Sciences). Seven-week-old $IFNAR^{-/-}$ mice were inoculated subcutaneously with 10-fold serial dilutions of GX015 (10^4–10^1 plaque forming units (PFUs)/mouse) and monitored for 14 days. Whole-blood samples of the mice inoculated with 10^2 PFUs of GX015 were collected daily in EDTA. The mice showing severe clinical signs were euthanized immediately, and several organs (heart, liver, spleen, lung, kidney, brain, thymus and inguinal and mesenteric lymph nodes) were collected. Tissues were homogenized in DMEM using a Tissue Lyser homogenizer (Qiagen). The viruses were released from whole-blood and homogenized tissues by performing three freeze/thaw cycles. Viral RNA was detected by quantitative real-time PCR (qRT-PCR) using the probe and primers target for S9 (Maan et al., 2015), and qRT-PCR was carried out with a HiScript II U^+ One Step qRT-PCR Probe Kit (Vazyme) with conditions of 55°C for 15 min, 95°C for 30 s, followed by 50 cycles of 95°C for 10 s and 60°C for 45 s on a QuantStudio 5 Real-Time PCR

System (Applied Biosystems, ABI). The amount of infectious virus was measured by the median tissue culture infective dose ($TCID_{50}$) method. Tissues from different organs were fixed in 10% buffered formalin (pH 7.2) for histopathological and immunohistochemical studies.

2.5 | Experimental infection of sheep with GX015

Three 6-month-old female small-tailed Han sheep were used in this study. The viral inoculum used for infection was passaged once in C6/36 cells and five times in BHK-21 cells. Two sheep were inoculated intravenously with GX015 at 10^5 $TCID_{50}$/sheep, and another sheep was employed as a control. The rectal temperature and clinical signs of each sheep were recorded and monitored daily for 14 days. Whole-blood in EDTA and serum were collected daily until the end of the experiment. Viral RNA was extracted from 200 μl of whole-blood with TRI reagent and detected by the qRT-PCR as described above. The collected sera were heat inactivated for 30 min at 56°C. The serum samples were analyzed with a commercially available BTV competition enzyme-linked immunosorbent assay (cELISA) kit (IDvet, France) according to the manufacturer's instructions, and a serum neutralization test was performed as described previously (Batten et al., 2012).

3 | RESULTS

3.1 | Viral isolation, identification and whole genome sequencing

The morphology of viral particles was observed on EM as spherical virions of approximately 70–80 nm in diameter without envelopes (Figure S1(a)). In addition, the observed virus specifically reacted with an anti-BTV VP7 Mab in IFA and plaque morphology analysis (Figures S1(b) and S1(c)). Furthermore, the infection of BHK-21 cells with the viruses was significantly blocked by BTV-20 reference strain antiserum. These results indicated that the virus isolated here was a BTV strain, which was classified as BTV-20. The strain was named BTV-20/GX015/China/2013, abbreviated as GX015.

The characteristics of the GX015 genome, including the length of each segment, deduced amino acid (aa) sequences and non-coding regions, are listed in Table S1. The 10 genomic segments of GX015 ranged in length from 822 bp (S10) to 3944 bp (S1), forming a whole genome of 19,176 bp. The 5′ and 3′ terminal hexanucleotides of all genomic segments were as follows: 5′-GTTAAA…ACTTAC-3′, corresponding to the highly conserved sequences previously identified in BTV genomes (Mertens & Sangar, 1985). The full-length nt sequences of S1–S10 have been submitted to GenBank under accession numbers OL333534 to OL333543.

3.2 | Phylogenetic analysis

Comparative analyses of S2/VP2 and S6/VP5 revealed that GX015 exhibited the closest relationships to BTV-20 strains at both the nt (91.0–91.1% for S2 and 92.6–92.7% for S6) and aa (95.3–95.4% for VP2 and 97.7–97.9% for VP5) levels; these homologies were significantly higher than those between GX015 and the BTV strains from any other serotypes (43.4–71.2% nt and 29.8–78.0% aa for S2/VP2, 57.6–79.5% nt and 56.0–93% aa for S6/VP5). In the phylogenetic trees of S2 and S6 (Figure 1), GX015 was also clustered together with BTV-20 strains to form a distinct, well-supported clade. These results demonstrated that GX015 belongs to BTV-20 and confirmed the preliminary identification result of VNT at the genetic level. Although S2 and S6 of GX015 shared high nt similarities (91.0 and 92.7%, respectively) with those of the BTV-20 reference strain RSArrrr/20, the similarities were much lower than those between other BTV-20 strains and RSArrrr/20 (99.9% for S2 and 99.9–100% for S6). Phylogenetic trees also showed that GX015 itself formed a separate sub-lineage within the BTV-20 clade, and other BTV-20 strains isolated from South Africa and Australia formed another distinct sub-lineage (Figure 1). These results indicated that GX015 is significantly divergent from the original South African reference strain and other BTV-20 strains, suggesting that GX015 represents a new topotype within BTV-20 strains based on the sequences of S2 and S6.

Although GX015 was clustered with BTV-20 strains in the phylogenetic trees based on S2 and S6, phylogenetic analyses of the other eight genomic segments revealed a significant difference. The majority of segments in the BTV genome show sequence variations correlated with the geographic origins of these segments and can be clustered into distinct groups (Maan et al., 2015; Maan et al., 2008; Maan et al., 2010). Here, S1, S3–S5 and S7–S10 of GX015 notably showed the highest nt identities with BTV strains originating from China, regardless of serotype. The phylogenetic trees based on these eight segments showed the existence of obviously separated clades (Figures 2 and 3): BTV strains are grouped exclusively based on eastern or western origin, and GX015 belongs to the Eastern group and clustered with most BTV strains isolated from China. Additionally, six (S1, S3–S5, S7 and S10) of the eight segments shared maximum nt identities of 98.2, 97.7, 97.7, 98.9, 98.1 and 98.9%, respectively, with the BTV-12 strain BTV12/PT/2003 isolated from Taiwan. In the phylogenetic trees based on the six segments (Figure 2), GX015 clustered together with BTV12/PT/2003 to form a unique branch within the Eastern group, indicating that they shared a common origin. These results demonstrated that S1, S3–S5 and S7–S10 of GX015 are of eastern origin and originated from Chinese BTV strains, most of which shared the same ancestor as the Taiwanese strain BTV-12/PT/2003.

3.3 | Infectivity and pathogenicity of GX015 in $IFNAR^{-/-}$ mice

$IFNAR^{-/-}$ mice are considered a good animal model for studying the pathogenesis, virulence and transmission of BTV (Calvo-Pinilla et al., 2010; Calvo-Pinilla et al., 2009; Marin-Lopez et al., 2016). To analyze the infectivity and pathogenicity of GX015, $IFNAR^{-/-}$ mice were subcutaneously inoculated with 10^4 PFUs of GX015. Starting at 3 dpi, the mice showed clinical signs characterized by reduced activity, a ruffled

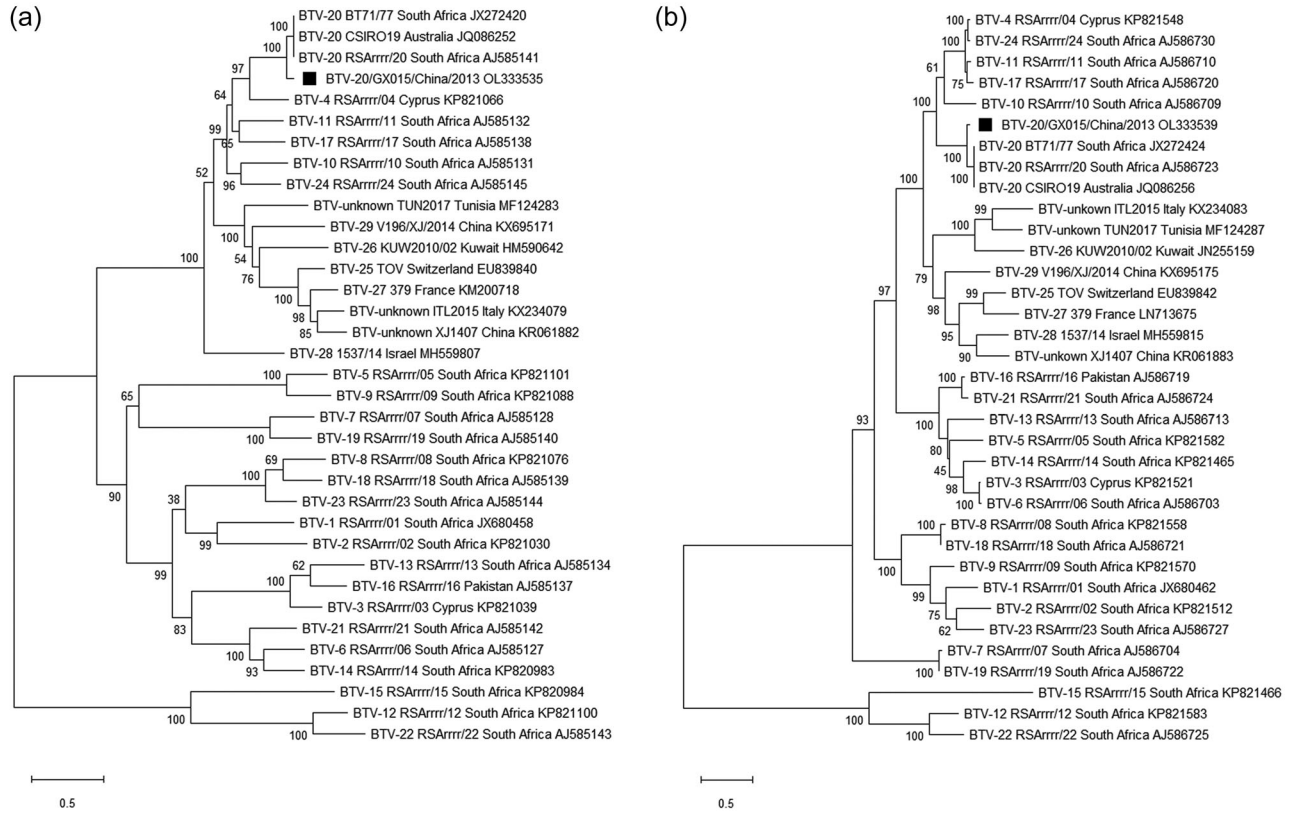

FIGURE 1 Phylogenetic analyses based on the genomic segments 2 (S2) and 6 (S6) of BTV-20/GX015/China/2013 (■) and bluetongue virus (BTV) reference strains from GenBank. Phylogenetic relationships of full-length S2 (A) and S6 (B) nucleotide sequences were inferred in MEGA X using the maximum likelihood (ML) method and tested by bootstrapping 1000 replicates. The best-fitted nucleotide substitution model of GTR+G+I was obtained for both S2 and S6 using the Bayesian Information Criterion (BIC). The following convention was used to identify sequences: BTV serotype_strain name_country (region)_GenBank accession number

TABLE 1 The qRT-PCR detection of viral RNA in the whole-blood and tissue samples of GX015-infected IFNAR$^{-/-}$ mice

Samples	2 dpi	3 dpi	4 dpi	5 dpi
Whole-blood	38.69 ± 0.50	30.26 ± 1.24	26.35 ± 2.51	21.55 ± 2.88
Heart	ND	32.72 ± 4.81	28.07 ± 1.99	25.70 ± 6.20
Liver	35.97 ± 2.60	26.91 ± 2.27	19.54 ± 3.28	14.38 ± 2.58
Spleen	34.47 ± 3.32	25.30 ± 1.31	20.42 ± 2.19	16.29 ± 1.64
Lung	ND	28.06 ± 2.31	23.27 ± 0.47	22.56 ± 2.54
Kidney	ND	29.71 ± 2.51	28.17 ± 3.40	22.67 ± 2.75
Brain	ND	31.66 ± 1.80	29.27 ± 4.32	24.16 ± 1.87
Thymus	ND	29.02 ± 2.74	33.03 ± 0.64	23.12 ± 0.49
Inguinal lymph node	ND	36.84 ± 1.39	32.48 ± 1.54	25.75 ± 1.70
Mesenteric lymph node	ND	35.68 ± 3.40	35.76 ± 1.84	27.87 ± 0.97

Results were expressed as the mean cycle threshold (Ct) values ($n = 4$) and standard deviations. Ct value > 40 was set as a standard negative result threshold. dpi, days post infection; ND, not detected.

hair coat, huddling tendency, hunched posture and apathy. Severe disease progression led to death starting at 4 dpi, and 100% of the mice died within 5 dpi (Figure 4(a)).

Viraemia and viral dissemination among different organs from the IFNAR$^{-/-}$ mice infected with 10^2 PFUs of GX015 were detected by qRT-PCR (Table 1). Viral RNA was first detected in whole-blood at 2 dpi, and the level of viraemia increased thereafter until the mice died. In addition, viral RNA was detected in the spleen and liver as early as 2 dpi, and by 3 dpi, viral RNA was also detected in the lung, heart, kidney, brain, thymus and inguinal and mesenteric lymph nodes. The

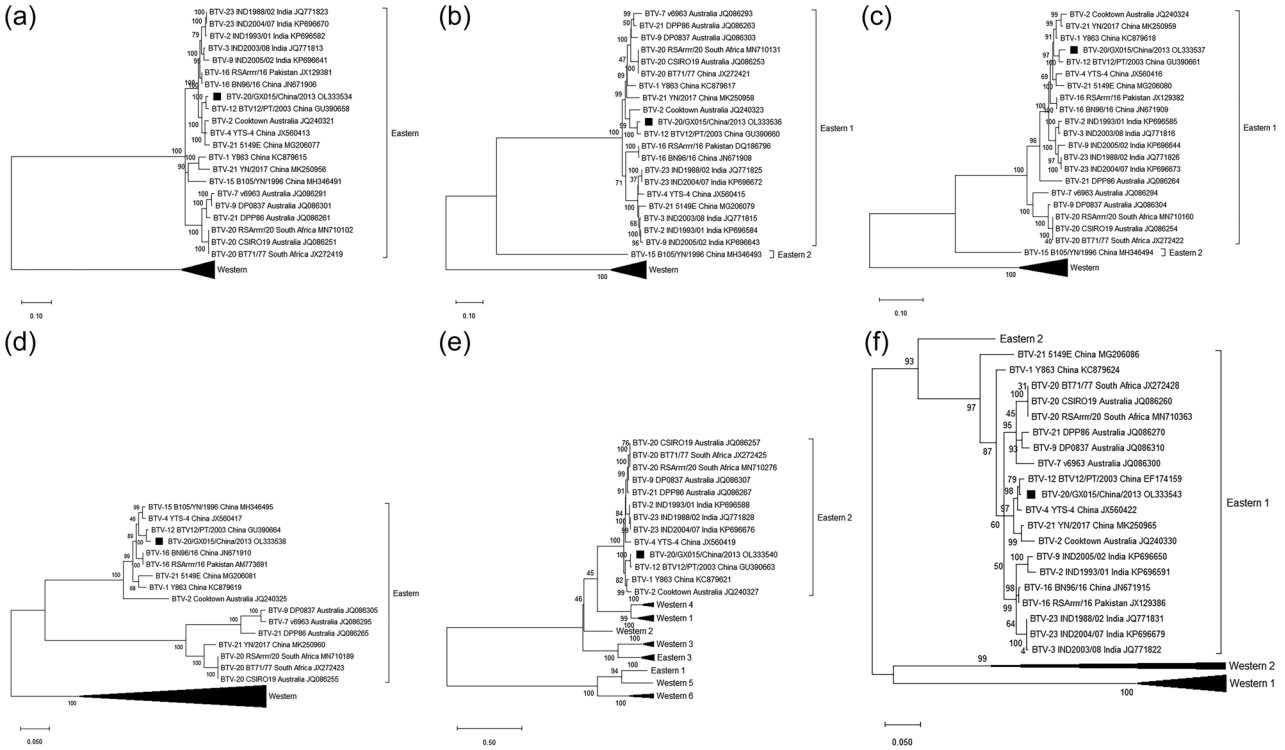

FIGURE 2 Phylogenetic analyses based on the genomic segments 1 (S1), 3–5 (S3–S5), 7 (S7) and 10 (S10) of BTV-20/GX015/China/2013 (■) and bluetongue virus (BTV) strains from GenBank. The phylogenetic relationship of full-length S1 (a), S3 (b), S4 (c), S5 (d), S7 (e) and S10 (f) nucleotide sequences were inferred in MEGA X using the maximum likelihood (ML) method and tested by bootstrapping 1000 replicates. The best-fitted nucleotide substitution models obtained for different genomic segments using the Bayesian Information Criterion (BIC) were GTR+G+I (S1, S2 and S6); T92+G+I (S3 and S5); TN93+G+I (S4 and S7); and T92+G (S10). Eastern and Western groups assigned as previously (Maan et al., 2015; Maan et al., 2008). The following convention was used to identify sequences: BTV serotype_strain name_country (region)_GenBank accession number

viral RNA content continued to increase thereafter until the mice died. Additionally, the titres of virus recovered from the whole-blood and tissue samples of GX015-infected mice were determined (Figure 4(b)). High virus titres were successfully detected in the whole-blood, heart, spleen, thymus, inguinal and mesenteric lymph nodes, lungs, liver, kidney and brain, and peaked before the mice died, which was consistent with the viral RNA level determined by qRT-PCR.

To examine the pathological lesions caused by GX015 in IFNAR$^{-/-}$ mice, histopathological examinations were performed on the different organs. The gross pathological alterations included widespread oedema, congestion and haemorrhages, especially in the spleen, lung, liver and lymph nodes. Additionally, the histopathological lesions caused by GX015 are shown in Figure 5: liver (Figure 5(a)), hepatocyte degeneration and necrosis, and centrilobular microvacuolations; spleen (Figure 5(b)), lymphoid depletion and extensive necrosis; lung (Figure 5(c)), interstitial pneumonia, mild proliferation of alveolar epithelial cells and inflammatory cell infiltration; kidney (Figure 5(d)), denaturation and necrosis of renal tubule epithelial cells; cerebrum (Figure 5(e)), degeneration of neuronal cells in the hippocampal dentate gyrus, with a small area of focal infiltration of glial cells; cerebellum (Figure 5(f)), partial Purkinje cell degeneration; thymus (Figure 5(g)), lymphoid depletion and necrosis, with the medulla and cortex becoming indistinguishable; and inguinal and mesenteric lymph nodes (Figures 5(h) and 5(i)), lymphoid depletion, necrosis and inflammatory cell infiltration. To confirm viral replication in the lesioned organs mentioned above, BTV-specific immunohistochemistry staining was performed. Clear immunoreactivity signs were detected in the liver, spleen, lung, kidney, cerebrum, cerebrum, thymus and inguinal and mesenteric lymph nodes of GX015-infected IFNAR$^{-/-}$ mice (Figure 6). These histopathological findings were similar to those observed in BTV-infected natural hosts (Calvo-Pinilla et al., 2009; Marin-Lopez et al., 2016; Sanchez-Cordon et al., 2010; Worwa et al., 2010).

3.4 | Infectivity and pathogenicity of GX015 in sheep

To determine the infectivity and pathogenicity of GX015 in the natural host, two sheep were intravenously inoculated with GX015 (10^5 $TCID_{50}$/sheep). The two GX015-inoculated sheep showed clinical manifestations, including a rise in rectal temperature (>40.0°C) at 2 or 3 dpi lasting for 2 days before the temperature decreased to a normal level (Figure 7(a)) and a decrease in appetite at 2–4 dpi. However, the sheep

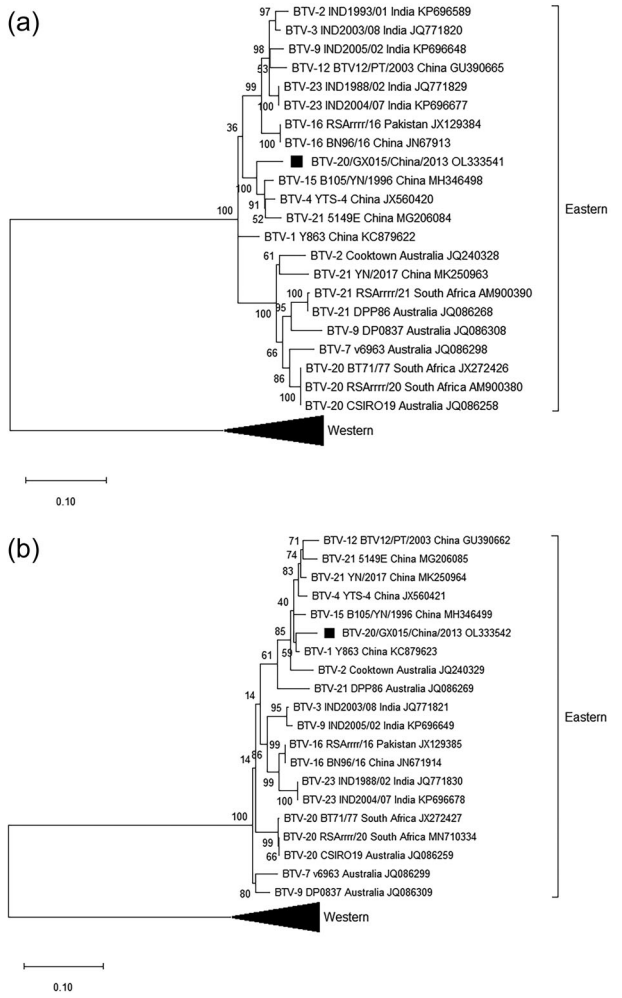

FIGURE 3 Phylogenetic analyses based on the genomic segments 8 (S8) and 9 (S9) of BTV-20/GX015/China/2013 (■) and bluetongue virus (BTV) strains from GenBank. The phylogenetic relationship of full-length S8 (a) and S9 (b) nucleotide sequences were inferred in MEGA X using the maximum likelihood (ML) method and tested by bootstrapping 1000 replicates. The best-fitted nucleotide substitution models obtained for different genomic segments using the Bayesian Information Criterion (BIC) were TN93+G+I (S8) and TN93+G (S9). Eastern and Western groups assigned as previously (Maan et al., 2015; Maan et al., 2008). The following convention was used to identify sequences: BTV serotype_strain name_country (region)_GenBank accession number

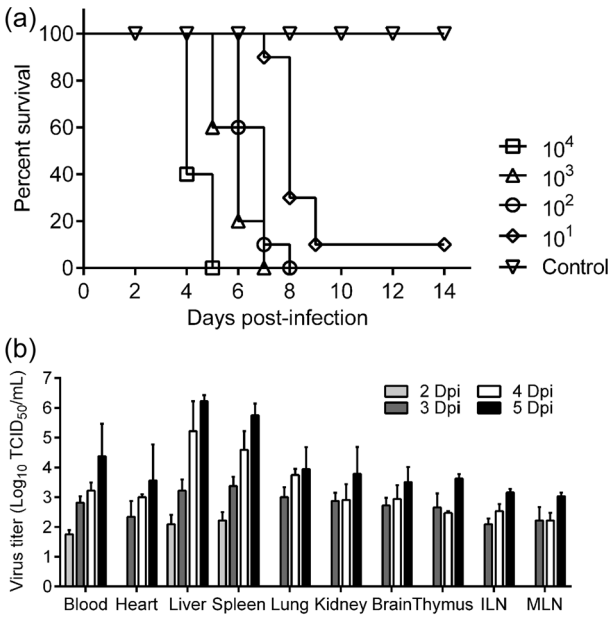

FIGURE 4 Seven-week-old $IFNAR^{-/-}$ mice were inoculated subcutaneously with BTV-20/GX015/China/2013 or DMEM as a control. (a) Survival rates of $IFNAR^{-/-}$ mice after inoculation with GX015. $IFNAR^{-/-}$ mice (10 mice per group) were subcutaneously inoculated with 10-fold serial dilutions (10^4 to 10^1 PFUs/mouse) of GX015 and observed for 14 days. (b) Viral titre in the whole-blood and tissue samples of the $IFNAR^{-/-}$ mice inoculated with 10^2 PFUs of GX015. Each point represents the mean value ($n = 4$), and standard deviations are shown as error bars. $IFNAR^{-/-}$ mice, the mice lacking the interferon receptor. ILN, inguinal lymph node; MLN, mesenteric lymph node

as control had no clinical signs. At 3 dpi, viraemia was observed in GX015-inoculated sheep through viral RNA detection by qRT-PCR and remained positive for 3 days; thereafter, no viral RNA was detected until the end of the experiment (Figure 7(b)). To confirm the propagation of GX015 in the sheep, viral RNA-positive whole-blood was used for virus isolation, and the homologous virus was successfully recovered and confirmed by S2 sequencing (data not shown). These results indicated that GX015 replicates effectively in sheep and causes clinical signs and viraemia at a dose of 10^5 $TCID_{50}$/sheep.

BTV seroconversion was detected in GX015-inoculated sheep at 5 dpi and remained positive throughout the experiment (Figure 7(c)). Virus-neutralizing antibodies (VNAs) were also detected at 5 dpi with serum dilutions of 1:8 and 1:16, and the titres reached peak values of 1:32 and 1:64 at 10 dpi, respectively (Figure 7(d)). No anti-BTV antibodies were detected in the control sheep throughout the experiment.

4 | DISCUSSION

In this study, we reported the whole genome sequencing and phylogenetic analyses of the first BTV-20 strain, BTV-20/GX015/China/2013, isolated in China and evaluated the infectivity and pathogenicity of the BTV-20 strain in $IFNAR^{-/-}$ mice and sheep. Phylogenetic analyses based on the sequences of S2/VP2 and S6/VP5 showed that GX015 clustered with BTV-20 strains and exhibited the highest sequence identities with these strains. VP2 is the main protein used to determine BTV serotype, and VP5 shows some correlation with BTV serotype by influencing the conformation of VP2 (Hassan et al., 2001; Maan, et al., 2007; Zhang et al., 2010). Therefore, GX015 belongs to BTV-20, and a VNT using BTV-20 reference strain antiserum also confirmed this classification. Both S2 and S6 exhibit variations within a single BTV serotype that reflect the geographic origins of isolates and/or segments and can be used to clearly group them as distinct topotypes (Maan et al., 2015; Maan et al., 2008; Maan et al., 2010; Yang et al., 2021).

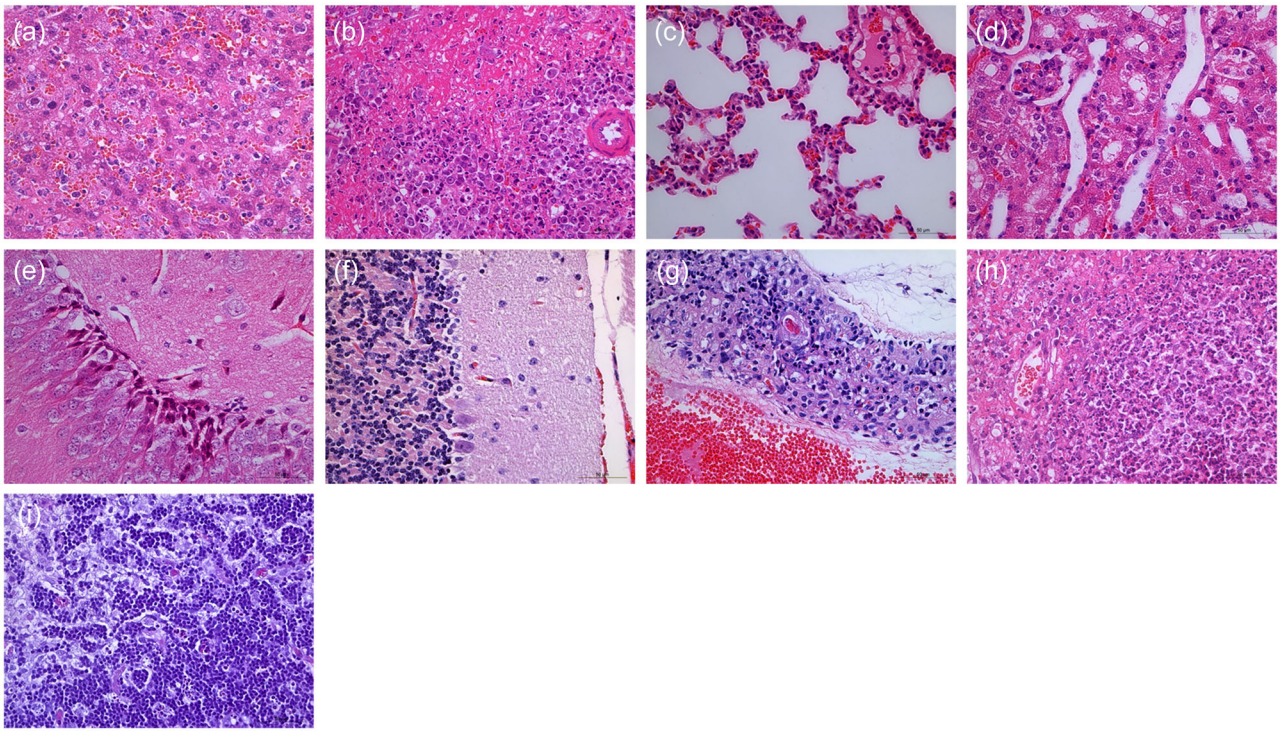

FIGURE 5 Histopathological lesions of the different tissue samples from GX015-infected IFNAR$^{-/-}$ mice. (a) Liver; (b) spleen; (c) lung; (d) kidney; (e) cerebrum; (f) cerebellum; (g) thymus; (h) inguinal lymph node; (i) mesenteric lymph node. Haematoxylin and eosin (h&e) stain; scale bar indicates 50 μm; IFNAR$^{-/-}$ mice, the mice lacking the interferon receptor

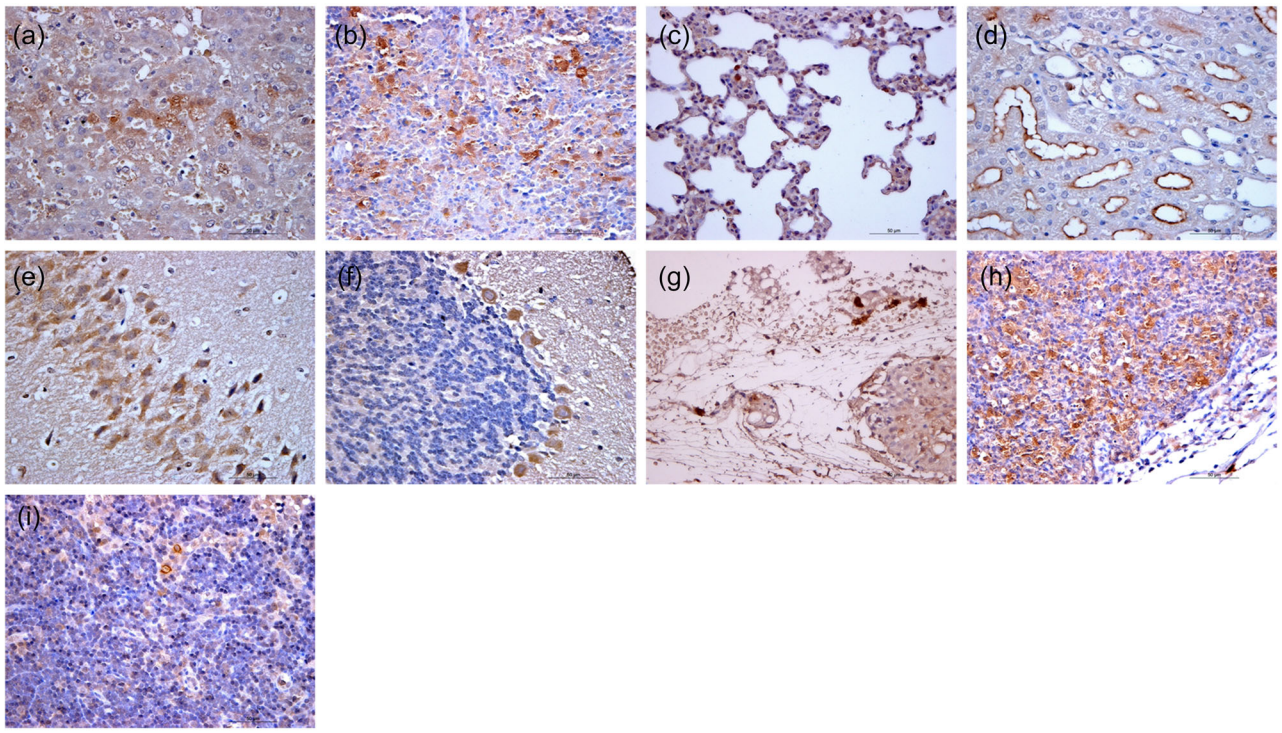

FIGURE 6 Immunohistochemical staining of the different tissue samples from GX015-infected IFNAR$^{-/-}$ mice. (a) Liver; (b) spleen; (c) lung; (d) kidney; (e) cerebrum; (f) cerebellum; (g) thymus; (h) inguinal lymph node; (i) mesenteric lymph node. Scale bar indicates 50 μm; IFNAR$^{-/-}$ mice, the mice lacking the interferon receptor

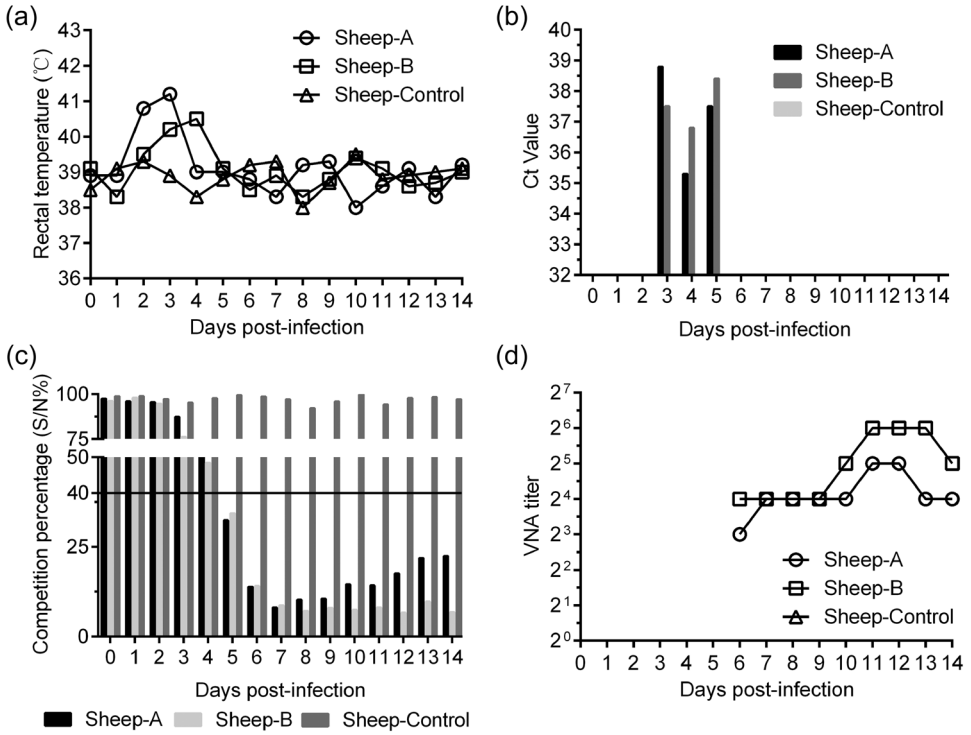

FIGURE 7 Sheep were inoculated intravenously with GX015 or DMEM as a control. (a) Rectal temperatures of GX015-inoculated sheep. (b) Viral RNA in the whole-blood of GX015-inoculated sheep was detected by qRT-PCR. Cycle threshold (Ct) values greater than 40 were considered negative. (c) Bluetongue virus (BTV) VP7-specific antibodies in the serum samples of GX015-inoculated sheep were detected by a commercially available competitive enzyme-linked immunosorbent assay (cELISA) kit, and the ratio of inhibition with percentage values less than 40% (indicated by horizontal black line) was considered positive. (d) Virus-neutralizing antibodies in the serum samples of GX015-inoculated sheep were detected by serum neutralization tests. The virus-neutralizing antibody (VNA) titre was expressed as the dilution ratio of serum

The BTV-20 strains isolated from South Africa and Australia clustered together to form a sub-lineage, and GX015 alone formed another sub-lineage; therefore, GX015 probably represents a new topotype within BTV-20 based on S2 and S6. Since BTV-20 has never been reported in China or other countries except for South Africa and Australia, and only a few BTV-20 strains are available in GenBank, further study is necessary to confirm this finding via identification and phylogenetic analyses of additional BTV-20 isolates.

Although GX015 has been identified as a BTV-20 strain, the S1, S3–S5, S7 and S10 of GX015 exhibited the maximum sequence similarities with that of a Taiwanese BTV-12 isolate and clustered together with it to form a separate branch within Eastern groups. In addition, both S8 and S9 of GX015 shared a higher sequence identity and a closer relationship with BTV strains from China, regardless of serotype. Thus, the 10 genomic segments of GX015 probably underwent reassortment, in which S2 and S6 of outer capsid proteins were derived from exotic BTV-20 strains (South Africa or Australia), while the remaining inner genomic segments were apparently of Chinese origin and most likely shared the same ancestor with a Taiwanese BTV-12 isolate. Unfortunately, due to a lack of continual surveillance of BTV throughout China or additional genome sequences of BTV-20 and BTV-12 strains, we could not determine any details about when or where a new serotype of BTV arose or underwent reassortment. Genomic segments of the members of the *Orbivirus* genus including BTV can undergo reassortment, resulting in a large number of new combinations (Golender et al., 2019; Qi et al., 2019; Shafiq et al., 2013; Shaw et al., 2013). These new reassortant viruses may exhibit different phenotypic characteristics than their parental viruses, which result in an increase or decrease in transmissibility or pathogenicity or the ability to infect a new host (Golender et al., 2019; Qi et al., 2019; Shafiq et al., 2013; Shaw et al., 2013).

IFNAR$^{-/-}$ mice are highly susceptible to BTV, and disease progression and pathogenesis induced in these mice closely mimic the typical characteristics of BTV in ruminants (Calvo-Pinilla et al., 2010; Calvo-Pinilla et al., 2009; Marin-Lopez et al., 2016). In this study, IFNAR$^{-/-}$ mice infected with GX015 developed clinical signs and histopathological lesions, and severe disease progression led to death. Furthermore, high viraemia levels and virus titres were detected in the whole-blood and tissue samples of GX015-infected mice, respectively, and the dissemination of GX015 in IFNAR$^{-/-}$ mice also followed the pattern of BTV infection recorded in natural host sheep (Darpel et al., 2007; Sanchez-Cordon et al., 2013; Worwa et al., 2010). Additionally, GX015 killed 90% of the infected mice at a dose as low as 10^1 PFUs/mouse, which was similar to the result with BTV-8 infection in IFNAR$^{-/-}$ mice at the same dose (Calvo-Pinilla et al., 2009). Notably, GX015 caused histopathological lesions in the cerebrum and cerebellum of the infected mice; viral RNA and infectious virus were also detected in the brain. Previous studies have shown that brain tissues collected

from BTV-8-infected sheep contain high levels of viral RNA (Worwa et al., 2010). BTV-8 exhibits enhanced virulence in cattle, and BTV-4 usually causes sub-clinical infections; the virulence difference between the two serotypes was maintained in IFNAR$^{-/-}$ mice, as observed in cattle (Barratt-Boyes & MacLachlan, 1994; Calvo-Pinilla et al., 2009; MacLachlan et al., 1990). Thus, GX015 is probably a highly virulent strain and likely exhibits strong virulence in natural hosts, in line with the severe disease and lesions it causes in IFNAR$^{-/-}$ mice.

GX015 was isolated from asymptomatic sentinel cattle, so we chose sheep as experimental animals to evaluate the infectivity and pathogenicity of GX015 in natural hosts. GX015 infection caused an increase in rectal temperature and a decrease in appetite in sheep. Viraemia was observed in GX015-infected sheep, and infectious virus was successfully recovered from whole-blood samples. Additionally, BTV VP7-specific antibodies and VNAs were detected in the serum samples of GX015-infected sheep. Therefore, GX015 replicates effectively and causes clinical signs in BTV natural host sheep. However, significant differences in the pathogenicity of GX015 between IFNAR$^{-/-}$ mice and sheep were observed. The possible factors responsible for these differences are as follows. First, sheep were infected with GX015 at a dose of 10^5 $TCID_{50}$/sheep, a significantly lower infectious dose than that needed with other BTV strains employed to infect sheep (Darpel et al., 2007; Sanchez-Cordon et al., 2013). Second, the viral inoculum of GX015 used for infection in sheep was passaged several times in different cell lines. Cell culture-adapted viruses retain a high replication capacity in cultured cell lines, but their virulence and pathogenicity in a natural host are likely affected. Therefore, whole-blood samples collected from BTV-infected animals are considered to be the first choice for BTV infection experiments in natural hosts (MacLachlan et al., 2008; Worwa et al., 2010). Third, the severity of disease induced by BTV differs markedly among infections in different ruminant species or breeds and even within the same ruminant species or breed when infected by different strains (Coetzee et al., 2014; Maclachlan et al., 2009). GX015 was isolated from asymptomatic sentinel cattle and exhibits mild pathogenicity in sheep infected with a low dose; however, it causes severe disease and death in IFNAR$^{-/-}$ mice. Therefore, determination of the pathogenicity of GX015 in other natural hosts requires further research. Additionally, considering that only two sheep were used in this study, subsequent experiments involving more animals are necessary. Based on the factors mentioned above, we will further investigate the infectivity and pathogenicity of GX015 in natural hosts, by changing the experimental parameters such as the increased infectious dose of virus in sheep, the replaced inoculum using whole-blood samples collected from GX015-infected sheep and the selected goats as experimental animals.

In summary, our study describes the isolation, identification, genomic characteristics and pathogenicity of the first recorded Chinese BTV-20 strain BTV-20/GX015/China/2013. The detailed results presented in this study are important for understanding the origin, genetic characteristics and pathogenicity of BTVs, as well as developing diagnostic methods and vaccines for the surveillance and prevention of BT.

ACKNOWLEDGMENTS

We acknowledge H.R. Liu and other animal caretakers (Department of Animal Experiment Services, Harbin Weike Biotechnology) for their support during the animal experiment. This work was supported by the National Natural Science Foundation of China under Grant number 32102651 and 31201941; and Inner Mongolia Autonomous Region Major Science and Technology Project under Grant number 2020ZD0006.

CONFLICT OF INTEREST

The authors declare that they have no conflict of interest.

ETHICS STATEMENT

All animal experiments were conducted using research protocols approved by the Committee on the Ethics of Animal Experiments of Harbin Veterinary Research Institute (HVRI) of the Chinese Academy of Agricultural Sciences (CAAS) (authorization No. 210104-01), and performed in accordance with the guidelines for experimental animals of the Ministry of Science and Technology (Beijing, China).

DATA AVAILABILITY STATEMENT

The data that support the findings of this study are available from the corresponding author upon reasonable request.

ORCID

Jianmin Wu https://orcid.org/0000-0003-0627-9383
Li Yu https://orcid.org/0000-0002-0386-204X

REFERENCES

Barratt-Boyes, S. M., & MacLachlan, N. J. (1994). Dynamics of viral spread in bluetongue virus infected calves. *Veterinary Microbiology*, *40*(3-4), 361–371. Retrieved from https://www.ncbi.nlm.nih.gov/pubmed/7941299. https://doi.org/10.1016/0378-1135(94)90123-6

Batten, C. A., Henstock, M. R., Bin-Tarif, A., Steedman, H. M., Waddington, S., Edwards, L., & Oura, C. A. (2012). Bluetongue virus serotype 26: Infection kinetics and pathogenesis in Dorset Poll sheep. *Veterinary Microbiology*, *157*(1-2), 119–124. Retrieved from https://www.ncbi.nlm.nih.gov/pubmed/22177889. https://doi.org/10.1016/j.vetmic.2011.11.033

Belhouchet, M., Mohd Jaafar, F., Firth, A. E., Grimes, J. M., Mertens, P. P., & Attoui, H. (2011). Detection of a fourth orbivirus non-structural protein. *PLoS One*, *6*(10), e25697. Retrieved from https://www.ncbi.nlm.nih.gov/pubmed/22022432. https://doi.org/10.1371/journal.pone.0025697

Calvo-Pinilla, E., Nieto, J. M., & Ortego, J. (2010). Experimental oral infection of bluetongue virus serotype 8 in type I interferon receptor-deficient mice. *Journal of General Virology*, *91*(Pt 11), 2821–2825. Retrieved from https://www.ncbi.nlm.nih.gov/pubmed/20719994. https://doi.org/10.1099/vir.0.024117-0

Calvo-Pinilla, E., Rodriguez-Calvo, T., Anguita, J., Sevilla, N., & Ortego, J. (2009). Establishment of a bluetongue virus infection model in mice that are deficient in the alpha/beta interferon receptor. *PLoS One*, *4*(4), e5171. Retrieved from https://www.ncbi.nlm.nih.gov/pubmed/19357779. https://doi.org/10.1371/journal.pone.0005171

Coetzee, P., vanVuuren, M., Venter, E. H., & Stokstad, M. (2014). A review of experimental infections with bluetongue virus in the mammalian host. *Virus Research*, *182*, 21–34. Retrieved from https://www.ncbi.nlm.nih.gov/pubmed/24462840. https://doi.org/10.1016/j.virusres.2013.12.044

Darpel, K. E., Batten, C. A., Veronesi, E., Shaw, A. E., Anthony, S., Bachanek-Bankowska, K., Kgosana, L., bin-Tarif, A., Carpenter, S., Müller-Doblies,

U. U., Takamatsu, H. H., Mellor, P. S., Mertens, P. P., & Oura, C. A. (2007). Clinical signs and pathology shown by British sheep and cattle infected with bluetongue virus serotype 8 derived from the 2006 outbreak in northern Europe. *The Veterinary Record*, *161*(8), 253–261. Retrieved from https://www.ncbi.nlm.nih.gov/pubmed/17720961. https://doi.org/10.1136/vr.161.8.253

Elbers, A. R., Backx, A., Ekker, H. M., van derSpek, A. N., & vanRijn, P. A. (2008). Performance of clinical signs to detect bluetongue virus serotype 8 outbreaks in cattle and sheep during the 2006-epidemic in The Netherlands. *Veterinary Microbiology*, *129*(1-2), 156–162. Retrieved from https://www.ncbi.nlm.nih.gov/pubmed/18164148. https://doi.org/10.1016/j.vetmic.2007.10.034

Elbers, A. R., Backx, A., Meroc, E., Gerbier, G., Staubach, C., Hendrickx, G., van derSpek, A., & Mintiens, K. (2008). Field observations during the bluetongue serotype 8 epidemic in 2006. I. Detection of first outbreaks and clinical signs in sheep and cattle in Belgium, France and the Netherlands. *Preventive Veterinary Medicine*, *87*(1-2), 21–30. Retrieved from https://www.ncbi.nlm.nih.gov/pubmed/18620767. https://doi.org/10.1016/j.prevetmed.2008.06.004

Golender, N., Eldar, A., Ehrlich, M., Khinich, Y., Kenigswald, G., Varsano, J. S., Ertracht, S., Abramovitz, I., Assis, I., Shlamovitz, I., Tiomkin, E., Yonay, E., Sharir, B., & Bumbarov, V. Y. (2019). Emergence of a novel reassortant strain of bluetongue serotype 6 in Israel, 2017: Clinical manifestations of the disease and molecular characterization. *Viruses*, *11*(7), Retrieved from https://www.ncbi.nlm.nih.gov/pubmed/31295819. https://doi.org/10.3390/v11070633

Hassan, S. H., Wirblich, C., Forzan, M., & Roy, P. (2001). Expression and functional characterization of bluetongue virus VP5 protein: Role in cellular permeabilization. *Journal of Virology*, *75*(18), 8356–8367. Retrieved from https://www.ncbi.nlm.nih.gov/pubmed/11507181. https://doi.org/10.1128/jvi.75.18.8356-8367.2001

Hofmann, M. A., Renzullo, S., Mader, M., Chaignat, V., Worwa, G., & Thuer, B. (2008). Genetic characterization of toggenburg orbivirus, a new bluetongue virus, from goats, Switzerland. *Emerging Infectious Diseases*, *14*(12), 1855–1861. Retrieved from https://www.ncbi.nlm.nih.gov/pubmed/19046507. https://doi.org/10.3201/eid1412.080818

Kumar, S., Stecher, G., Li, M., Knyaz, C., & Tamura, K. (2018). MEGA X: Molecular evolutionary genetics analysis across computing platforms. *Molecular Biology and Evolution*, *35*(6), 1547–1549. Retrieved from https://www.ncbi.nlm.nih.gov/pubmed/29722887. https://doi.org/10.1093/molbev/msy096

Larkin, M. A., Blackshields, G., Brown, N. P., Chenna, R., McGettigan, P. A., McWilliam, H., Valentin, F., Wallace, I. M., Wilm, A., Lopez, R., Thompson, J. D., Gibson, T. J., & Higgins, D. G. (2007). Clustal W and Clustal X version 2.0. *Bioinformatics*, *23*(21), 2947–2948. Retrieved from https://www.ncbi.nlm.nih.gov/pubmed/17846036. https://doi.org/10.1093/bioinformatics/btm404

Lorusso, A., Sghaier, S., Di Domenico, M., Barbria, M. E., Zaccaria, G., Megdich, A., Portanti, O., Seliman, I. B., Spedicato, M., Pizzurro, F., Carmine, I., Teodori, L., Mahjoub, M., Mangone, I., Leone, A., Hammami, S., Marcacci, M., & Savini, G. (2018). Analysis of bluetongue serotype 3 spread in Tunisia and discovery of a novel strain related to the bluetongue virus isolated from a commercial sheep pox vaccine. *Infection, Genetics and Evolution*, *59*, 63–71. Retrieved from https://www.ncbi.nlm.nih.gov/pubmed/29386141. https://doi.org/10.1016/j.meegid.2018.01.025

Maan, N. S., Maan, S., Belaganahalli, M., Pullinger, G., Montes, A. J., Gasparini, M. R., Guimera, M., Nomikou, K., & Mertens, P. P. (2015). A quantitative real-time reverse transcription PCR (qRT-PCR) assay to detect genome segment 9 of all 26 bluetongue virus serotypes. *Journal of Virological Methods*, *213*, 118–126. Retrieved from https://www.ncbi.nlm.nih.gov/pubmed/25486080. https://doi.org/10.1016/j.jviromet.2014.11.012

Maan, S., Maan, N. S., Belaganahalli, M. N., Rao, P. P., Singh, K. P., Hemadri, D., Putty, K., Kumar, A., Batra, K., Krishnajyothi, Y., Chandel, B. S., Reddy, G. H., Nomikou, K., Reddy, Y. N., Attoui, H., Hegde, N. R., & Mertens, P. P. (2015). Full-genome sequencing as a basis for molecular epidemiology studies of bluetongue virus in India. *Plos One*, *10*(6), e0131257. Retrieved from https://www.ncbi.nlm.nih.gov/pubmed/26121128. https://doi.org/10.1371/journal.pone.0131257

Maan, S., Maan, N. S., Nomikou, K., Batten, C., Antony, F., Belaganahalli, M. N., Samy, A. M., Reda, A. A., Al-Rashid, S. A., El Batel, M., Oura, C. A., & Mertens, P. P. (2011). Novel bluetongue virus serotype from Kuwait. *Emerging Infectious Diseases*, *17*(5), 886–889. Retrieved from https://www.ncbi.nlm.nih.gov/pubmed/21529403. https://doi.org/10.3201/eid1705.101742

Maan, S., Maan, N. S., Ross-smith, N., Batten, C. A., Shaw, A. E., Anthony, S. J., Samuel, A. R., Darpel, K. E., Veronesi, E., Oura, C. A., Singh, K. P., Nomikou, K., Potgieter, A. C., Attoui, H., vanRooij, E., vanRijn, P., De Clercq, K., Vandenbussche, F., …, & Mertens, P. P. (2008). Sequence analysis of bluetongue virus serotype 8 from the Netherlands 2006 and comparison to other European strains. *Virology*, *377*(2), 308–318. Retrieved from https://www.ncbi.nlm.nih.gov/pubmed/18570969. https://doi.org/10.1016/j.virol.2008.04.028

Maan, S., Maan, N. S., Samuel, A. R., Rao, S., Attoui, H., & Mertens, P. P. C. (2007). Analysis and phylogenetic comparisons of full-length VP2 genes of the 24 bluetongue virus serotypes. *Journal of General Virology*, *88*(Pt 2), 621–630. Retrieved from https://www.ncbi.nlm.nih.gov/pubmed/17251581. https://doi.org/10.1099/vir.0.82456-0

Maan, S., Maan, N. S., vanRijn, P. A., vanGennip, R. G., Sanders, A., Wright, I. M., Batten, C., Hoffmann, B., Eschbaumer, M., Oura, C. A., Potgieter, A. C., Nomikou, K., & Mertens, P. P. (2010). Full genome characterisation of bluetongue virus serotype 6 from the Netherlands 2008 and comparison to other field and vaccine strains. *PLoS One*, *5*(4), e10323. Retrieved from https://www.ncbi.nlm.nih.gov/pubmed/20428242. https://doi.org/10.1371/journal.pone.0010323

Maan, S., Rao, S., Maan, N. S., Anthony, S. J., Attoui, H., Samuel, A. R., & Mertens, P. P. (2007). Rapid cDNA synthesis and sequencing techniques for the genetic study of bluetongue and other dsRNA viruses. *Journal of Virological Methods*, *143*(2), 132–139. Retrieved from https://www.ncbi.nlm.nih.gov/pubmed/17433453. https://doi.org/10.1016/j.jviromet.2007.02.016

Maclachlan, N. J. (2011). Bluetongue: History, global epidemiology, and pathogenesis. *Preventive Veterinary Medicine*, *102*(2), 107–111. Retrieved from https://www.ncbi.nlm.nih.gov/pubmed/21570141. https://doi.org/10.1016/j.prevetmed.2011.04.005

MacLachlan, N. J., Crafford, J. E., Vernau, W., Gardner, I. A., Goddard, A., Guthrie, A. J., & Venter, E. H. (2008). Experimental reproduction of severe bluetongue in sheep. *Veterinary Pathology*, *45*(3), 310–315. Retrieved from https://www.ncbi.nlm.nih.gov/pubmed/18487487. https://doi.org/10.1354/vp.45-3-310

Maclachlan, N. J., Drew, C. P., Darpel, K. E., & Worwa, G. (2009). The pathology and pathogenesis of bluetongue. *Journal of Comparative Pathology*, *141*(1), 1–16. Retrieved from https://www.ncbi.nlm.nih.gov/pubmed/19476953. https://doi.org/10.1016/j.jcpa.2009.04.003

MacLachlan, N. J., Jagels, G., Rossitto, P. V., Moore, P. F., & Heidner, H. W. (1990). The pathogenesis of experimental bluetongue virus infection of calves. *Veterinary Pathology*, *27*(4), 223–229. Retrieved from https://www.ncbi.nlm.nih.gov/pubmed/2169663. https://doi.org/10.1177/030098589002700402

Marcacci, M., Sant, S., Mangone, I., Goria, M., Dondo, A., Zoppi, S., vanGennip, R. G. P., Radaelli, M. C., Cammà, C., vanRijn, P. A., Savini, G., & Lorusso, A. (2018). One after the other: A novel Bluetongue virus strain related to Toggenburg virus detected in the Piedmont region (North-western Italy), extends the panel of novel atypical BTV strains. *Transboundary and Emerging Diseases*, *65*(2), 370–374. Retrieved from https://www.ncbi.nlm.nih.gov/pubmed/29392882. https://doi.org/10.1111/tbed.12822

Marin-Lopez, A., Bermudez, R., Calvo-Pinilla, E., Moreno, S., Brun, A., & Ortego, J. (2016). Pathological characterization Of IFNAR(-/-) mice

infected with bluetongue virus serotype 4. *International Journal of Biological Sciences*, *12*(12), 1448–1460. Retrieved from https://www.ncbi.nlm.nih.gov/pubmed/27994510. https://doi.org/10.7150/ijbs.14967

Mertens, P. P., & Sangar, D. V. (1985). Analysis of the terminal sequences of the genome segments of four orbiviruses. *Virology*, *140*(1), 55–67. Retrieved from https://www.ncbi.nlm.nih.gov/pubmed/2981457. https://doi.org/10.1016/0042-6822(85)90445-3

Potgieter, A. C., Page, N. A., Liebenberg, J., Wright, I. M., Landt, O., & vanDijk, A. A. (2009). Improved strategies for sequence-independent amplification and sequencing of viral double-stranded RNA genomes. *Journal of General Virology*, *90*(Pt 6), 1423–1432. Retrieved from https://www.ncbi.nlm.nih.gov/pubmed/19264638. https://doi.org/10.1099/vir.0.009381-0

Qi, Y., Wang, F., Chang, J., Zhang, Y., Zhu, J., Li, H., & Yu, L. (2019). Identification and complete-genome phylogenetic analysis of an epizootic hemorrhagic disease virus serotype 7 strain isolated in China. *Archives of Virology*, *164*(12), 3121–3126. Retrieved from https://www.ncbi.nlm.nih.gov/pubmed/31538253. https://doi.org/10.1007/s00705-019-04412-9

Ratinier, M., Caporale, M., Golder, M., Franzoni, G., Allan, K., Nunes, S. F., Armezzani, A., Bayoumy, A., Rixon, F., Shaw, A., & Palmarini, M. (2011). Identification and characterization of a novel non-structural protein of bluetongue virus. *PLoS Pathogens*, *7*(12), e1002477. Retrieved from https://www.ncbi.nlm.nih.gov/pubmed/22241985. https://doi.org/10.1371/journal.ppat.1002477

Rushton, J., & Lyons, N. (2015). Economic impact of Bluetongue: A review of the effects on production. *Veterinaria Italiana*, *51*(4), 401–406. Retrieved from https://www.ncbi.nlm.nih.gov/pubmed/26741252. https://doi.org/10.12834/VetIt.646.3183.1

Sanchez-Cordon, P. J., Pleguezuelos, F. J., Perez de Diego, A. C., Gomez-Villamandos, J. C., Sanchez-Vizcaino, J. M., Ceron, J. J., Tecles, F., Garfia, B., & Pedrera, M. (2013). Comparative study of clinical courses, gross lesions, acute phase response and coagulation disorders in sheep inoculated with bluetongue virus serotype 1 and 8. *Veterinary Microbiology*, *166*(1-2), 184–194. Retrieved from https://www.ncbi.nlm.nih.gov/pubmed/23849094. https://doi.org/10.1016/j.vetmic.2013.05.032

Sanchez-Cordon, P. J., Rodriguez-Sanchez, B., Risalde, M. A., Molina, V., Pedrera, M., Sanchez-Vizcaino, J. M., & Gomez-Villamandos, J. C. (2010). Immunohistochemical detection of bluetongue virus in fixed tissue. *Journal of Comparative Pathology*, *143*(1), 20–28. Retrieved from https://www.ncbi.nlm.nih.gov/pubmed/20156627. https://doi.org/10.1016/j.jcpa.2009.12.017

Savini, G., Puggioni, G., Meloni, G., Marcacci, M., Di Domenico, M., Rocchigiani, A. M., Spedicato, M., Oggiano, A., Manunta, D., Teodori, L., Leone, A., Portanti, O., Cito, F., Conte, A., Orsini, M., Cammà, C., Calistri, P., Giovannini, A., & Lorusso, A. (2017). Novel putative Bluetongue virus in healthy goats from Sardinia, Italy. *Infection, Genetics and Evolution*, *51*, 108–117. Retrieved from https://www.ncbi.nlm.nih.gov/pubmed/28341545. https://doi.org/10.1016/j.meegid.2017.03.021

Shafiq, M., Minakshi, P., Bhateja, A., Ranjan, K., & Prasad, G. (2013). Evidence of genetic reassortment between Indian isolate of bluetongue virus serotype 21 (BTV-21) and bluetongue virus serotype 16 (BTV-16). *Virus Research*, *173*(2), 336–343. Retrieved from https://www.ncbi.nlm.nih.gov/pubmed/23353779. https://doi.org/10.1016/j.virusres.2013.01.009

Shaw, A. E., Ratinier, M., Nunes, S. F., Nomikou, K., Caporale, M., Golder, M., Allan, K., Hamers, C., Hudelet, P., Zientara, S., Breard, E., Mertens, P., & Palmarini, M. (2013). Reassortment between two serologically unrelated bluetongue virus strains is flexible and can involve any genome segment. *Journal of Virology*, *87*(1), 543–557. Retrieved from https://www.ncbi.nlm.nih.gov/pubmed/23097432. https://doi.org/10.1128/JVI.02266-12

Stewart, M., Hardy, A., Barry, G., Pinto, R. M., Caporale, M., Melzi, E., Hughes, J., Taggart, A., Janowicz, A., Varela, M., Ratinier, M., & Palmarini, M. (2015). Characterization of a second open reading frame in genome segment 10 of bluetongue virus. *Journal of General Virology*, *96*(11), 3280–3293. Retrieved from https://www.ncbi.nlm.nih.gov/pubmed/26290332. https://doi.org/10.1099/jgv.0.000267

Sun, E. C., Huang, L. P., Xu, Q. Y., Wang, H. X., Xue, X. M., Lu, P., Li, W. J., Liu, W., Bu, Z. G., & Wu, D. L. (2016). Emergence of a Novel Bluetongue Virus Serotype, China 2014. *Transboundary and Emerging Diseases*, *63*(6), 585–589. Retrieved from https://www.ncbi.nlm.nih.gov/pubmed/27597166. https://doi.org/10.1111/tbed.12560

vanGennip, R. G., van deWater, S. G., & vanRijn, P. A. (2014). Bluetongue virus nonstructural protein NS3/NS3a is not essential for virus replication. *PLoS One*, *9*(1), e85788. Retrieved from https://www.ncbi.nlm.nih.gov/pubmed/24465709. https://doi.org/10.1371/journal.pone.0085788

Worwa, G., Hilbe, M., Chaignat, V., Hofmann, M. A., Griot, C., Ehrensperger, F., Doherr, M. G., & Thur, B. (2010). Virological and pathological findings in Bluetongue virus serotype 8 infected sheep. *Veterinary Microbiology*, *144*(3-4), 264–273. Retrieved from https://www.ncbi.nlm.nih.gov/pubmed/20153937. https://doi.org/10.1016/j.vetmic.2010.01.011

Wouda, W., Roumen, M. P., Peperkamp, N. H., Vos, J. H., vanGarderen, E., & Muskens, J. (2008). Hydranencephaly in calves following the bluetongue serotype 8 epidemic in the Netherlands. *The Veterinary Record*, *162*(13), 422–423. Retrieved from https://www.ncbi.nlm.nih.gov/pubmed/18375990. https://doi.org/10.1136/vr.162.13.422-b

Yang, H., Gu, W., Li, Z., Zhang, L., Liao, D., Song, J., Shi, B., Hasimu, J., Li, Z., Yang, Z., Zhong, Q., & Li, H. (2021). Novel putative bluetongue virus serotype 29 isolated from inapparently infected goat in Xinjiang of China. *Transboundary and Emerging Diseases*, *68*(4), 2543–2555. Retrieved from https://www.ncbi.nlm.nih.gov/pubmed/33190404. https://doi.org/10.1111/tbed.13927

Zhang, X., Boyce, M., Bhattacharya, B., Zhang, X., Schein, S., Roy, P., & Zhou, Z. H. (2010). Bluetongue virus coat protein VP2 contains sialic acid-binding domains, and VP5 resembles enveloped virus fusion proteins. *Proceeding of the National Academy of Sciences of the United States of America*, *107*(14), 6292–6297. Retrieved from https://www.ncbi.nlm.nih.gov/pubmed/20332209. https://doi.org/10.1073/pnas.0913403107

Zientara, S., Sailleau, C., Viarouge, C., Hoper, D., Beer, M., Jenckel, M., Hoffmann, B., Romey, A., Bakkali-Kassimi, L., Fablet, A., Vitour, D., & Breard, E. (2014). Novel bluetongue virus in goats, Corsica, France, 2014. *Emerging Infectious Diseases*, *20*(12), 2123–2125. Retrieved from https://www.ncbi.nlm.nih.gov/pubmed/25418049. https://doi.org/10.3201/eid2012.140924

SUPPORTING INFORMATION

Additional supporting information may be found in the online version of the article at the publisher's website.

How to cite this article: Qi, Y., Wang, F., Chang, J., Jiang, Z., Sun, C., Lin, J., Wu, J., & Yu, L. (2022). Genetic characteristics and pathogenicity of the first bluetongue virus serotype 20 strain isolated in China. *Transboundary and Emerging Diseases*, 1–11. https://doi.org/10.1111/tbed.14555